

## **Efficient and accurate computations of phase-changing flows in Thermal Vapor Compressor system**

\*Daeho Min<sup>1)</sup>, Hyeongjun Kim<sup>1)</sup>, Hoon Lee<sup>2)</sup> and Chongam Kim<sup>3)</sup>

<sup>1), 3)</sup> *Department of Aerospace Engineering,  
Seoul National Univ. Seoul 151-744, Korea*

<sup>2)</sup> *Thermal and fluid research team, Corporate R&D Institute, Doosan Heavy  
Industries & Construction, Youngin, 39-3, Korea*

<sup>3)</sup> [chongam@snu.ac.kr](mailto:chongam@snu.ac.kr)

### **ABSTRACT**

Thermal Vapor Compressor (TVC) is a major device in Multiple-Effect Distiller (MED) system which desalinates sea water. Accurate prediction of entrainment performance of TVC is an important issue in the design process of MED system. At the same time, complex flow physics, such as shock-shear layer interaction and phase-changing process around shock-train region, makes it difficult to provide reliable and accurate computed solutions. In this paper, we carry out reliable and accurate computations of such flows with our baseline numerical schemes. As an equation of states for water and steam, IAPWS-97 and a regression model of Multi-parametric Equation of State (MEOS) are used to retain numerical accuracy as well as computational efficiency. Also, adaptive mesh refinement technique is employed to resolve local shock-train and its interaction with shear layer more accurately. By using above numerical methods, we present the numerical results of phase-changing flows in TVC system. Numerical results are compared with those of single-phase flow computations and experimental data. Based on the computed solutions and comparisons, we examine the local flow physics which plays a key role in determining the performance of TVC system.

### **1. INTRODUCTION**

The desalination technology has become an important issue nowadays because water shortage is still a problem in many countries around the world. In the past, most

---

<sup>1)</sup> Ph.D. student, Department of Aerospace Engineering, Seoul National University

<sup>2)</sup> Research Engineer, *Thermal and fluid research team, Corporate R&D Institute, Doosan Heavy Industries & Construction*

<sup>3)</sup> Professor, Department of Aerospace Engineering, Seoul National University, Corresponding author

of desalination plant used MSF(Multi Stage Flashing) type device, which can guarantee an enormous capacity but suffers from low efficiency. However, by introducing TVC(Thermal Vapor Compressor) which entrains the low pressure steam with shear force produced from supersonic and subsonic flow, MED(Multi Effect Distiller) type plant has become more energy-efficient and cost-competitive.

The entrainment ratio, which is dominant parameter defined as  $\dot{\omega} = \dot{m}_{suction} / \dot{m}_{motive}$  in TVC system, is directly related with desalination amount of MED system. So, accurate prediction of entrainment ratio of TVC system is important in the design process of MED system. But, complex physical phenomena, such as shock-shear layer interaction and phase changing process around shock train region, makes it very difficult to provide reliable and accurate computed solutions.

Regarding the numerical simulation of flow fields around TVC system, majority of CFD simulations reported in the literature assumed the working fluids as ideal gas(Chung *et al.*<sup>1</sup> Sharifi *et al.*<sup>2</sup>, T.Sriveerakul *et al.*<sup>3</sup>), which are known to be reasonable only in low operating pressure. Also, phase changing process should be taken into account to describe the real flow physics and to predict the system performance accurately. Some research considered phase changing effect with a growth rate of droplet.(Sharifi *et al.*<sup>5</sup>)

The focus of this paper is on the simulation of phase changing flows in TVC system and accurate prediction of system performance. We used our baseline numerical scheme AUSMPW+ which is known to be robust and accurate for single- and multi-phase shock capturing. To describe the real fluid properties of water and steam, IAPWS-97 and a regression model of Multi-parametric Equation of State(MEOS) are used to retain numerical accuracy and computational efficiency. Also, adaptive mesh refinement technique is employed to resolve local shock-train physics and mixing region more accurately. Our numerical results are then compared with those of single-phase flow computations and experimental data conducted by Doosan Heavy Industries. Finally, we explain the local flow physics which plays an important role in determining the performance of TVC system based on computed solution.

## 2. Governing equations

Our computation is based on homogeneous equilibrium model (HEM) with mass fraction to describe two-phase flow. Hence, the governing equations consist of mixture mass, momentum, and energy conservation laws with one-phase mass-conservation law. And governing equations are converted from conservative form to primitive form to apply the real fluid equation of states explicitly. So, two-dimensional Navier-Stokes system that adopted in this research can be written in computational coordinates as follows:

$$\frac{\Gamma_e}{J} \frac{\partial Q_p}{\partial \tau} + \frac{\partial E}{\partial \xi} + \frac{\partial F}{\partial \eta} = D + S_{phase}, \quad (1)$$

where  $\Gamma_e$  indicates conversion matrix from conservative foam to primitive foam. The

primitive variable vector  $Q_p$  and  $\xi$ -directional inviscid flux vector  $E$  are defined by

$$Q_p = [p \quad u \quad v \quad w \quad T \quad Y_1]^T,$$

$$E = \left[ \rho_m U \quad \rho_m u U + \xi_x p \quad \rho_m v U + \xi_y p \quad \rho_m w U + \xi_z p \quad \rho_m H U \quad \rho_m Y_1 U \right]^T.$$

Here,  $p$ ,  $\rho_m$  and  $H$  are the pressure, mixture density and mixture total enthalpy, respectively.  $Y_1$  stands for the mass fraction of gas phase and  $U$  is the contravariant velocity vector normal to interface of control volume.  $D$  is viscous flux and  $S_{phase}$  is the phase change source term.

In HEM, the definition of mixture density  $\rho_m$  is calculated with Amagat's law

$$\rho_m = 1 / \sum_i Y_i / \rho_i(p, T). \quad (2)$$

Here,  $\rho_i$  is the density of  $i$ -th fluid. In this research,  $\rho_i$  would be gas phase density or liquid phase density which can be calculated with function of pressure and temperature. The pressure and temperature within the computational cell are same for liquid and gas phase by dynamic and thermal equilibrium assumption.

### 3. Numerical methods

#### 3.1 Phase change model

The phase change source term is defined via a simplified non-equilibrium finite rate form as follows:

$$S_{phase} = \frac{1}{J} \left[ 0 \quad 0 \quad 0 \quad 0 \quad 0 \quad \dot{m}_{evaporation} \quad -\dot{m}_{condensation} \right]^T, \quad (2)$$

where  $\dot{m}_{evaporation}$  is the evaporation rate of vapor being generated from liquid in the region which the local pressure is less than the saturation pressure. Conversely,  $\dot{m}_{condensation}$  is the condensation rate for liquid phase back from vapor phase in the region which the local pressure exceeds the saturation pressure. The temperature variation is considered via saturation pressure. In flow fields around TVC system, shock-train region will experience phase changing phenomena by abrupt change of pressure and temperature. Therefore, phase change phenomena in flow fields around TVC system is similar to cavitation phenomena which phase change is governed by local pressure and saturation pressure. Hence, we used the following phase change source term which is similar to that of Merkle's model<sup>6</sup>:

$$\dot{m}_{evaporation} = C_{evaporation} \frac{\max(p_v - p, 0)}{p} \rho_l \alpha_l, \quad \dot{m}_{condensation} = C_{condensation} \frac{\max(p - p_v, 0)}{p} \rho_v \alpha_v, \quad (3)$$

where  $C_{evaporation}$  and  $C_{condensation}$  are empirical coefficient. Our numerical test confirms that  $10^5$  for both coefficients are adequate.

### 3.2 Equation of States

The NIST database, which employs Multi parametric Equation Of States (MEOS), is widely used due to its accuracy and wide applicable pressure and temperature range. But it requires huge computational cost because residual term of Helmholtz energy to compute the properties consists of many polynomials. Furthermore, it requires non-linear solver to compute the density such as Newton-Raphson method because pressure is function of density and temperature.

Recently, IAPWS (International Association for the Properties of Water and Steam) published IAPWS-97 formulation, which can compute the properties via Gibbs free energy as a function of pressure and temperature. Hence, it doesn't need non-linear solver to compute the density. So it can make numerical solver about 17 times faster comparing to MEOS in simple computation.

But, employing the IAPWS-97 formulation as equation of states still needs to improve the efficiency for complex problem or 3D computation. So we made a regression model of MEOS with piecewise polynomial functions. Figure 1 shows pressure contour of inviscid bump problem and table 1 shows total elapsed time for simulation. Three types of EOS provide identical results, which indicate that employment of regression model as EOS can retain the accuracy with improved efficiency.

Table 1 Elapsed time comparison to solve the inviscid bump problem

EOS	MEOS	IAPWS-97	Regression model
Elapsed time(sec)	1272.85	74.77	12.95
Normalized time	98	5.77	1

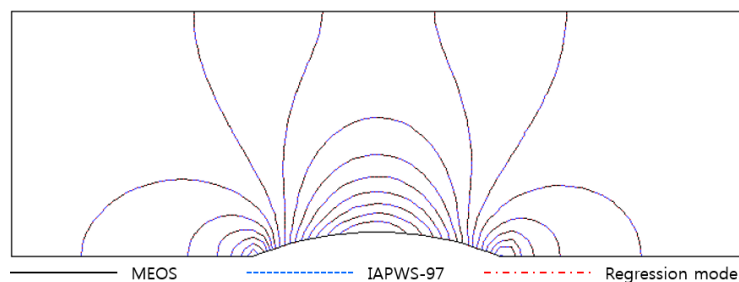


Fig. 1 Pressure contour comparison by varying equation of states

### 3.3 Generalization of Shock-Discontinuity Sensing Term

The two-phase AUSMPW+ scheme which has been developed in ref.7 employed shock discontinuity sensing term to control the numerical dissipation near the shock as follows:

$$\Pi_{1/2}^* = \min\left(\frac{\bar{p}_L}{\bar{p}_R}, \frac{\bar{p}_R}{\bar{p}_L}\right), \quad \bar{p}_{L,R} = 1 / \left( \frac{\alpha_{1,1/2}}{n_1 p_{L,R}} + \frac{1 - \alpha_{1,1/2}}{n_2 (p_{L,R} + p_c)} \right), \quad (4)$$

where  $\alpha_{1,1/2}$  is the volume fraction of gas phase at a cell interface that can be obtained from geometrical information or cell interface pressure, temperature, and mass fraction. But equation (4) is valid on limited type of equation of states such as ideal gas EOS, Tait's EOS and Peng-Robinson EOS. Hence, shock discontinuity sensing term should be modified for general type of equation of states as follows:

$$\Pi_{1/2}^{**} = \min\left(\frac{\bar{p}_L^*}{\bar{p}_R^*}, \frac{\bar{p}_R^*}{\bar{p}_L^*}\right), \quad \bar{p}_{L,R}^* = p_{L,R} + \frac{1}{2} \rho_{m,1/2} c_{m,1/2}^2 \quad (4)$$

Table 2 shows the behavior of shock discontinuity sensing term in 1-D shock relation by varying Mach number and mass fraction. Shock discontinuity sensing term  $\Pi$  is original form of ref.8 that is proposed for aerodynamic application. To make shock discontinuity sensing term work properly, it should have similar order of value regardless of mass fraction. But, the value of original form  $\Pi$  is significantly affected by mass fraction due to large difference of density between water and steam. By contrast, modified form  $\Pi^*$  and  $\Pi^{**}$  provide well-scaled values throughout the whole range of mass fraction. Therefore,  $\Pi^*$  and  $\Pi^{**}$  can be used consistently for all mixture flow regardless density and speed of sound. But again,  $\Pi^{**}$  can be applicable to general type of EOS, whereas  $\Pi^*$  is valid only on limited type of EOS,

Table 2 Inverse values of the shock discontinuity sensing term for the 1-D shock relation

P <sub>L</sub> = 101325Pa	M <sub>L</sub> =1.5			M <sub>L</sub> =2.0			M <sub>L</sub> =6.0		
	1/Π <sub>1/2</sub>	1/Π* <sub>1/2</sub>	1/Π** <sub>1/2</sub>	1/Π <sub>1/2</sub>	1/Π* <sub>1/2</sub>	1/Π** <sub>1/2</sub>	1/Π <sub>1/2</sub>	1/Π* <sub>1/2</sub>	1/Π** <sub>1/2</sub>
Y <sub>1</sub> =0.0 (pure liquid)	6565	3.188	1.625	15756	6.250	2.500	183812	62.250	18.498
Y <sub>1</sub> =10 <sup>-8</sup>	4836	2.612	1.539	12683	5.226	2.414	156147	53.03	18.41
Y <sub>1</sub> =10 <sup>-7</sup>	8.243	1.229	1.002	2495	1.833	1.644	64413	22.47	17.64
Y <sub>1</sub> =10 <sup>-6</sup>	2.426	2.065	1.003	4.844	2.786	1.007	5213	2.754	9.980
Y <sub>1</sub> =10 <sup>-5</sup>	2.266	2.229	1.020	4.069	3.831	1.049	44.86	5.753	1.703
Y <sub>1</sub> =10 <sup>-4</sup>	2.251	2.248	1.164	4.005	3.981	1.394	36.56	23.91	5.665
Y <sub>1</sub> =10 <sup>-3</sup>	2.249	2.249	1.592	3.999	3.997	2.420	35.90	34.13	17.52
Y <sub>1</sub> =10 <sup>-2</sup>	2.250	2.250	1.801	3.999	3.999	2.921	35.84	35.66	23.32
Y <sub>1</sub> =10 <sup>-1</sup>	2.254	2.254	1.831	4.009	4.009	2.994	35.95	35.93	24.16
Y <sub>1</sub> =1.0 (pure gas)	2.458	2.458	1.858	4.500	4.500	3.059	41.83	41.83	25.02

### 3.4 Spatial discretization scheme

The flow fields around TVC system contains strong shock and expansion wave with shear layer interaction. So AUSMPW+, which is well known for its accuracy and robustness on shock instability, is used as spatial discretization scheme.

### 3.5 Other numerical methods

In this research, cell by cell adaptive mesh refinement technique is used to resolve shock-train and mixing region more accurately. And effects of turbulent mixing are taken into account by employing  $k-\omega$  SST model and  $k-\varepsilon$  model with compressibility correction.

## 4. Numerical results

In this section, numerical results of TVC system will be presented. The geometries of TVC were taken from those which were experimented by Doosan Heavy Industries. Before conduct two-phase calculation, ideal gas and single-phase (steam) computation will be presented to examine its feasibility. Then two-phase computation will be presented and compared with ideal gas and single-phase computations. Then turbulence model comparison and mesh adaptation result will be presented.

The boundary conditions of primitive nozzle and suction nozzle are imposed as total pressure boundary, whereas discharge outlet is imposed as static pressure boundary. We tested 6 different configures of TVC system, which are operating on different pressure condition, to verify the feasibility of our numerical method. Figure 2 shows an example of mesh configuration used in this study, and table 3 shows the operating pressure condition.

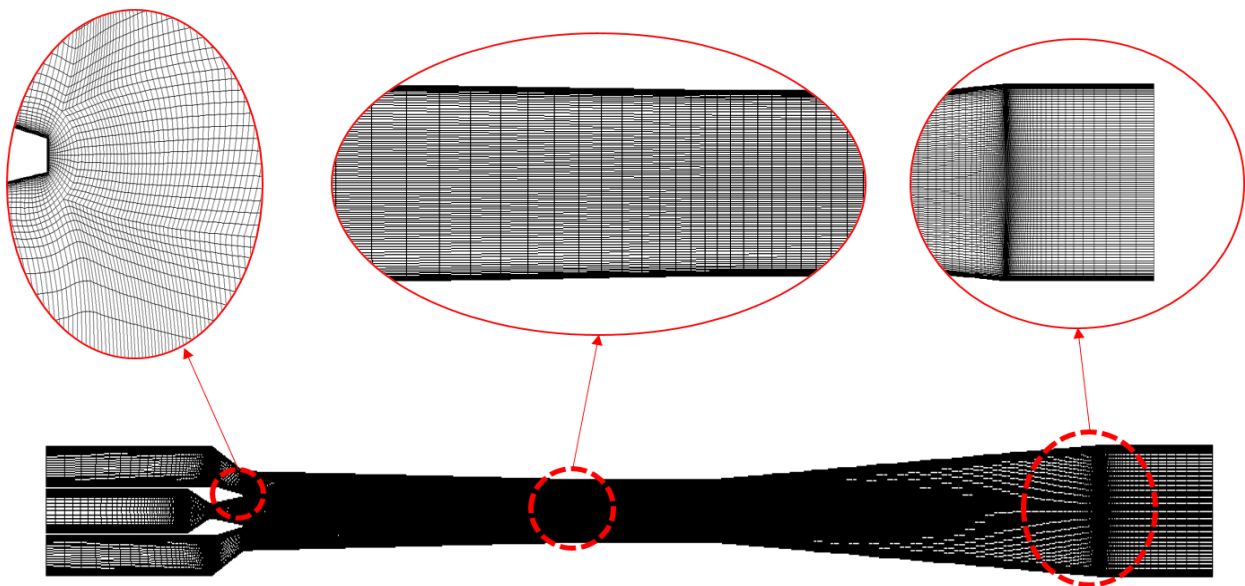


Fig. 2 Calculation domain and detailed view for computation

**Table 3 Operating condition of test cases**

	Case1	Case2	Case3	Case4	Case5	Case6
Primitive pressure(Bar)	2.5	3.4	5.968	9.6	13.3	15
Suction pressure(Bar)	0.167	0.170	0.252	0.163	0.141	0.148
Discharge pressure(Bar)	0.300	0.306	0.614	0.302	0.273	0.277

#### 4.1 Ideal gas and single-phase computation

In this section, feasibility of ideal gas or single-phase computation will be examined to predict system performance of TVC. The table 4 and table 5 are comparison of entrainment performance in ideal gas and single-phase computation, respectively. All data are normalized with experimental data due to confidential problem. Both table indicate that ideal gas or single-phase computation are inappropriate to predict the entrainment performance of TVC system. Although some case matched well in entrainment ratio such as case 6 in ideal gas computation, but it is still inaccurate for mass flow rate on motive and suction nozzle. Only case 4 in single-phase computation showed reasonable accuracy. Also, it should be noticed that case5 predicts reversed flow at suction nozzle on both computation.

**Table 4 Entrainment performance comparison in ideal gas case**

	Motive mass flow rate	Suction mass flow rate	E.R	E.R error
Case1	1.304	0.301	0.231	76.9%
Case2	1.268	0.524	0.414	58.6%
Case3	1.215	0.578	0.476	52.4%
Case4	1.247	0.752	0.603	39.7%
Case5	1.273	-0.123	-0.097	reversed flow
Case6	1.327	1.327	0.999	0%

**Table 5 Entrainment performance comparison in single-phase case**

	Motive mass flow rate	Suction mass flow rate	E.R	E.R error
Case1	1.004	0.194	0.193	80.7%
Case2	1.009	0.165	0.164	83.6%
Case3	0.931	0.974	1.047	4.6%
Case4	0.959	0.144	0.150	84.9%
Case5	0.982	-0.339	-0.346	reversed flow
Case6	1.048	0.302	0.286	71.4%

#### 4.2 Two-phase computation

In this section, two-phase computation results will be presented to improve the accuracy of numerical solution. Table 6 shows the entrainment performance

comparison, which indicates that numerical accuracy can be substantially enhanced with two-phase computation. Especially case 5, which predicted reversed flow in ideal gas or in single-phase computation, matched well experimental data.

Previous research<sup>4</sup> denotes that shear force between primitive and suction nozzle flows induces entrainment effect in flow fields of TVC system. Indeed, exact prediction on supersonic flows of primitive nozzle and on shear mixing are important to predict TVC system performance.

Figure 3 shows comparison of temperature distribution between single-phase and two-phase computation. As observed, temperature distribution in two-phase computation is above minimum acceptable limit (273.15K), whereas single-phase computation can be dropped below it in many places. Indeed, two-phase computation can exclude the unphysical region where single-phase computation allowed, and can describe the shock strength more close to reality. Figure 4 is comparison of temperature contour, in which gray portion in single-phase computation indicates unphysical region.

Table 6 Entrainment performance comparison in two-phase case

	Motive mass flow rate	Suction mass flow rate	E.R	E.R error
Case1	0.977	0.954	0.976	2.44%
Case2	0.979	0.905	0.925	7.45%
Case3	0.922	0.973	1.055	-5.54%
Case4	0.947	0.915	0.966	3.41%
Case5	0.981	0.881	0.960	4.00%
Case6	0.989	0.954	0.964	3.57%

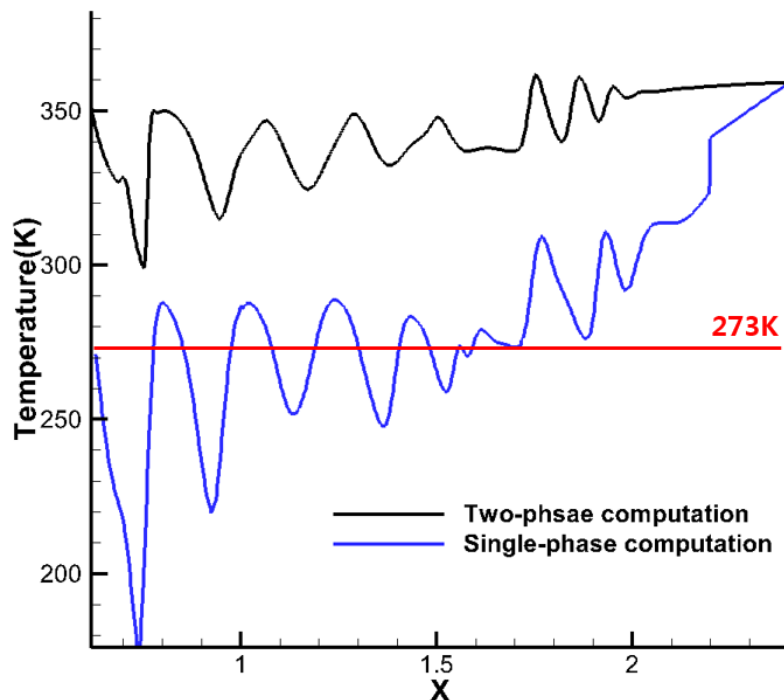


Fig. 3 Temperature distribution along the centerline in case 3

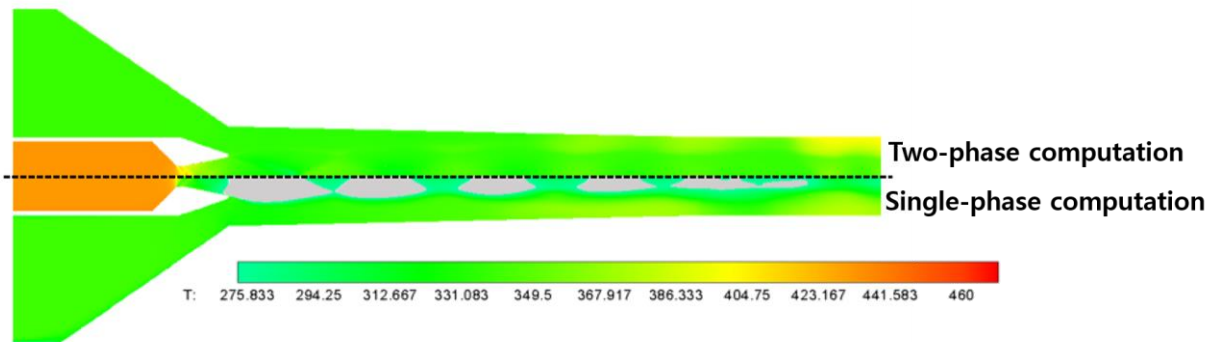


Fig. 4 Temperature contour comparison between two-phase and single-phase computation

Generally, expansion fan conserve the total enthalpy, but increase the kinetic energy of flow. Accordingly, flow should lose a certain amount of heat, but this heat is consumed in condensation process. Hence, temperature drop in two-phase computation is smaller than in single-phase computation. Also, difference of heat capacity between liquid and gas phase would be related on results. Indeed, it need more heat to make temperature variation in liquid phase than in gas phase, because its heat capacity is substantially larger.

Similarly, pressure rise in two-phase computation is small compared to single-phase case. Indeed, a certain portion of pressure rise due to shock wave is consumed by evaporation process. Figure 5-(a) shows this tendency more clearly, and consequently, the strength of shock wave and expansion fan are weakened in two-phase computation as Figure 5-(b). Figure 6, which shows the Mach number contour, supplement this difference.

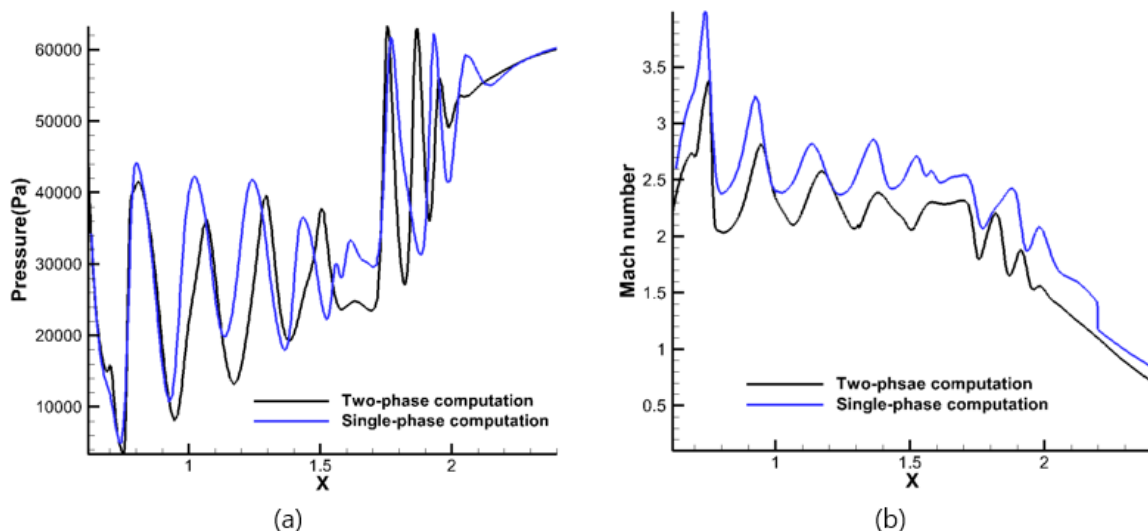


Fig. 5 Comparison of pressure(a) and mach number(b) distribution along to the centerline

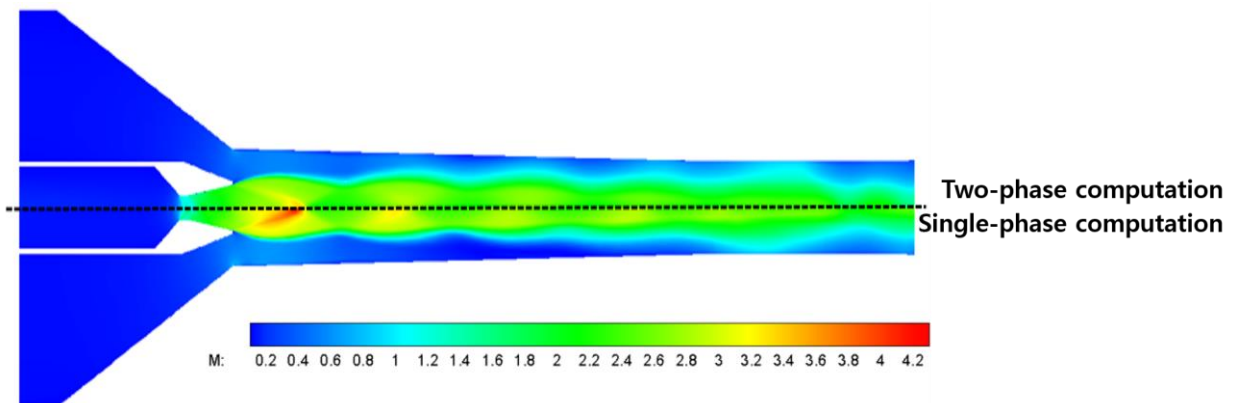


Fig. 6 Mach number contour comparison

#### 4.3 Turbulence model consideration

The key physics of flow fields around TVC is not only phase changing phenomena in shock-train region, but shear mixing near the primitive nozzle exit. Thus choice of turbulence model is important, so numerical results of 2 turbulence models,  $k-\omega$  SST and  $k-\varepsilon$  model, are computed and compared in table 7. As observed,  $k-\omega$  SST model showed more accurate results than  $k-\varepsilon$  model.

Figure 7 compares turbulent kinetic energy in case 1 and case2. As observed, turbulent kinetic energy is partially increased by shock wave, but  $k-\omega$  SST model predicts this interaction more shapely. It indicates that  $k-\omega$  SST model predicts shock-shear layer interaction more strongly than  $k-\varepsilon$  model. This interaction increases dissipation around shock-train region, so  $k-\omega$  SST model yields more diffusive results as Figure 8.

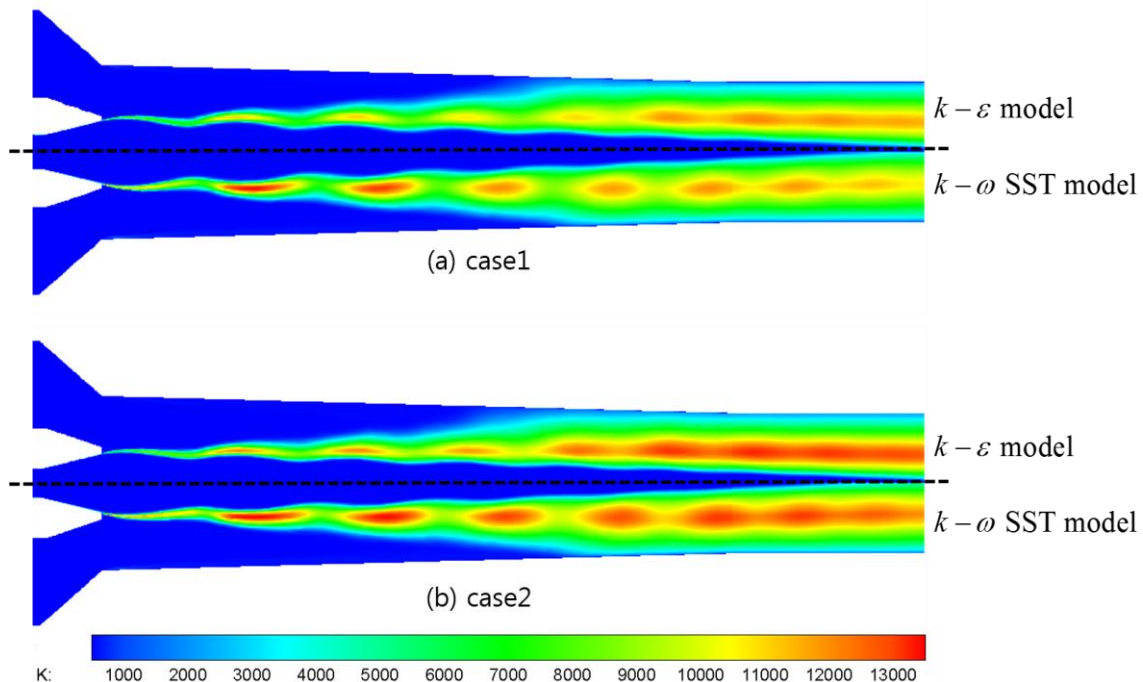


Fig 7. Turbulent kinetic energy contour comparison between turbulence models

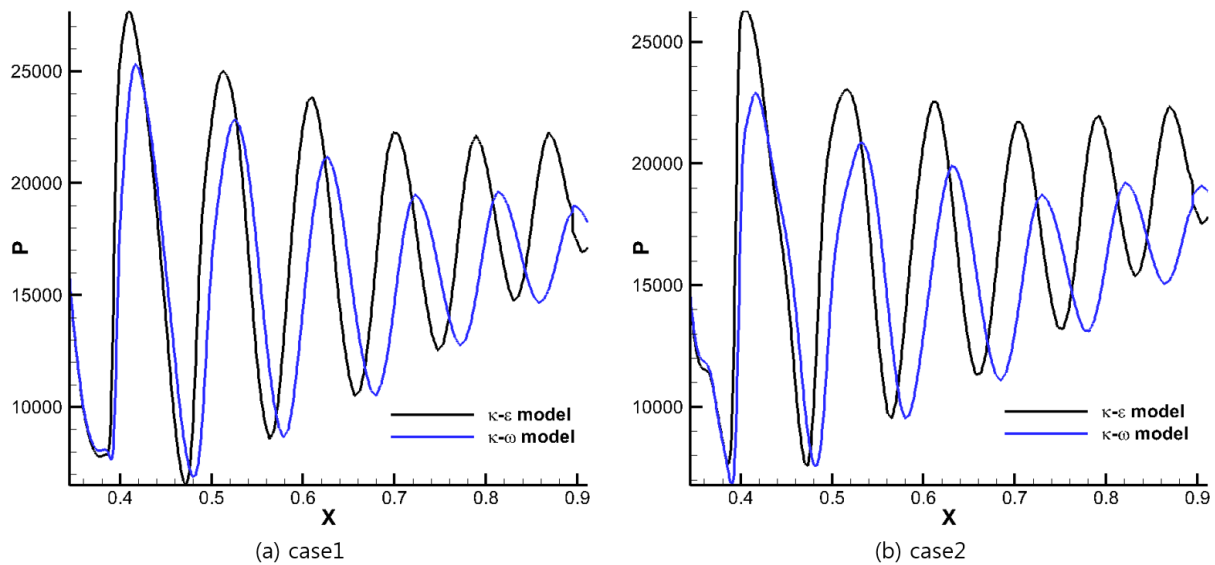


Fig 8. Pressure comparison along to the centerline

Table 7 Entrainment ratio comparison with turbulence model

	$k-\omega SST$	$k-\varepsilon$
Case1	0.977	0.576
Case2	0.925	0.516

#### 4.4 Adaptive mesh refinement

Figure 9 shows the example of variation of entrainment ratio with computing iteration by using adaptive mesh refinement. The initial coarse grid (30,000 cells) provides inaccurate result, which estimates about 40% lower comparing to experimental data even in two-phase computation. But adaptive mesh refinement technique can improve the numerical accuracy, and is summarized in table 8.

The reason is that excessive numerical dissipation induced by coarse mesh decays shock-train region widely as figure 10 which shows turbulent viscosity contour. As observed, turbulent viscosity in coarse mesh is substantially larger, so shock-train region is relatively confined compared to AMR result. Figure 11, which represents Mach number contour comparison, shows grid dependency clearly.

Table 8 Enhancement of numerical result by using AMR technique in two-phase computation

	Coarse mesh	AMR results
Entrainment ratio error	-45%	-2.3%
Number of cells	33,000	50,400

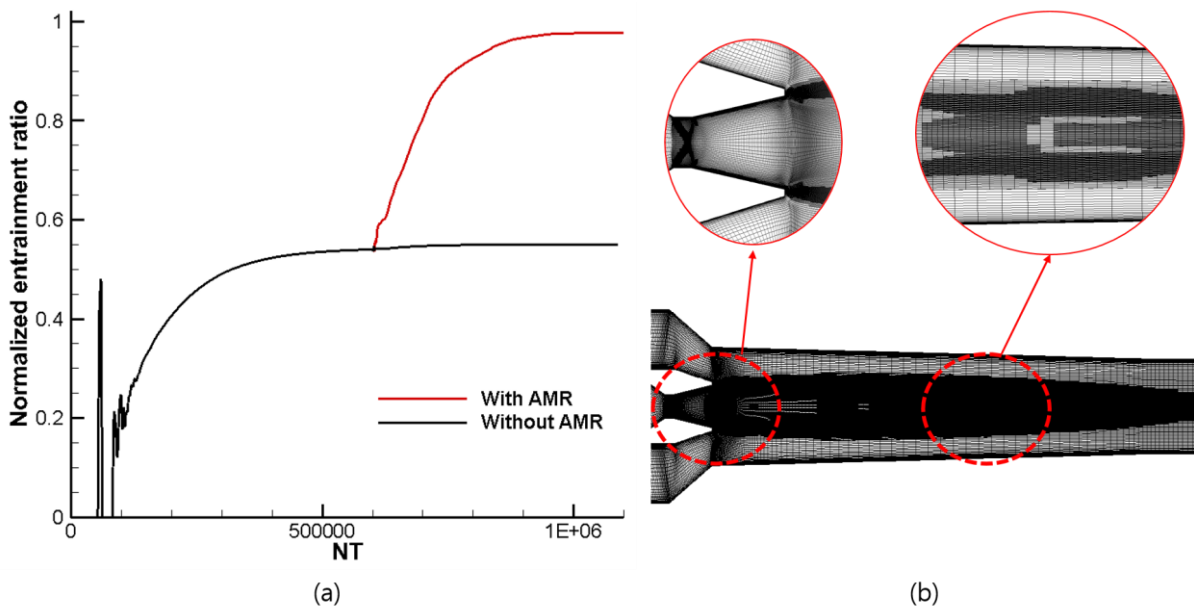


Fig 9. Converging history comparison(a) and refinement result(b)

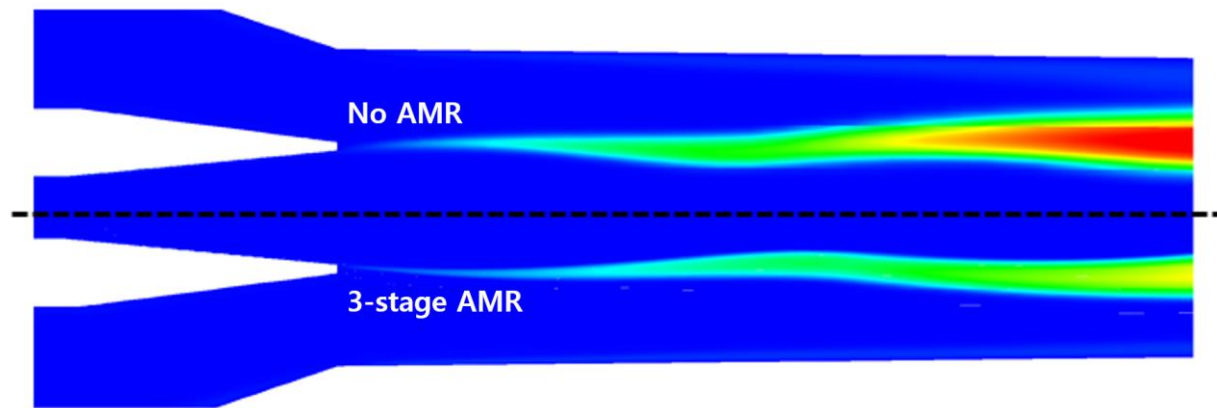


Fig 10. Turbulent viscosity comparison with and without AMR

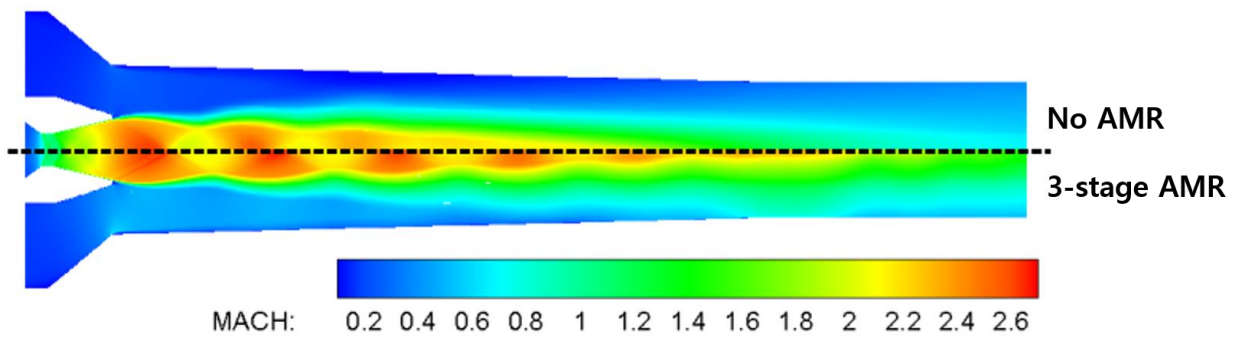


Fig 11. Mach number contour comparison with and without AMR

## 5. CONCLUSIONS

In this research, a set of numerical computations are conducted to predict entrainment performance of TVC system. In order to describe the properties of water and steam, MEOS, IAPWS-97 formulation and regression model of MEOS are successfully implemented. Next, shock discontinuity sensing term of AUSMPW+ scheme were modified to make it applicable for any types of equation of states. The phase change process was modeled via a simplified non-equilibrium finite rate form, which evaporation and condensation rate are proportional to pressure difference between local pressure and saturation pressure. And in order to resolve the shock-train region more accurately, adaptive mesh refinement technique was employed.

The numerical computation using ideal gas, which is known to be acceptable for low operating pressure, was examined to verify its feasibility. Predicted entrainment performance or mass flow rate on primitive and suction nozzle were not accurate. And this situation was not so far different in single-phase computation, either.

On the other hand, two-phase computation provided satisfactory results. The main reason is that ideal gas or single phase computation permits unphysical region, where temperature is dropped below triple point temperature (273.15K). In contrast, two-phase computation exclude this region via phase changing process, and describe the shock strength more close to physical reality.

Additionally, two turbulence models,  $k-\omega$  SST and  $k-\varepsilon$  model, were compared to choose adequate one to describe the shear mixing near primitive nozzle exit. In comparison,  $k-\omega$  SST model showed stronger shock-shear layer interaction. It means decaying of shock-train region due to shear mixing in  $k-\omega$  SST model is stronger than in  $k-\varepsilon$  model. And it leads to more accurate results comparing to experimental data. Finally, adaptive mesh refinement results, which have conducted to increase spatial accuracy, are presented. With adaptive mesh refinement technique, we obtained more accurate solution than in coarse mesh by resolving shock-train and shear-layer region more exactly.

## REFERENCES

- Hyomin Jeong, Tony Utomo, Myoungkuk Ji, Younghun Lee, Gyeonghwan Lee and Hanshik Chung, (2009), "CFD analysis of flow phenomena inside thermos vapor compressor influenced by operating conditions and converging duct angles", Journal of Mechanical Science and Technology, **23**, 2366-2375
- Navid Sharifi, Ramin Kouhikamali, S.M.A.Noori Rahim Abadi, (2013) "CFD simulation of supersonic jet behavior inside thermos compressors at different converging angles", World Congress on Desalination and Water, Tianjin, China
- T.Sriveerakul, S. Aphornratana and K.Chunnanond, (2007), "Performance prediction of steam ejector using computational fluid dynamics: Part 1. Validation of CFD results", International Journal of Thermal Science, **46**, 812-822
- T.Sriveerakul, S. Aphornratana and K.Chunnanond, (2007), "Performance prediction of steam ejector using computational fluid dynamics: Part 2. Flow structure of steam ejector influenced by operating pressures and geometries", International Journal of

Thermal Science, **46**, 823-833

Navid Sharifi, Masoud Boroomand, Majid Sharifi, (2013), "Numerical assessment of steam nucleation on thermodynamic performance of steam ejectors", Applied Thermal Engineering, **52**, 449-459

Merkle, C.L., Feng J.Z. and Buelow, P.E.Q,(1998), "Computational Modeling of Dynamics of Sheet Cavitation", Proceeding of 3<sup>rd</sup> International Symposium on Cavitation, Grenoble

Ihm, S. and C. Kim, (2008), "Computations of Homogeneous Equilibrium Two-phase Flows with Accurate and Efficient Shock-stable Schemes", AIAA Journal, **46**, 3012-3037

Kyu Hong Kim, Chongam Kim, and Oh-Hyun Rho, (2001), "Methods for the Accurate Computations of Hypersonic Flows, Part I. AUSMPW+ scheme", Journal of Computational Physics, **174**(1), 38-80